The 2022 WMO Technical Conference on Meteorological and Environmental Instruments and Methods of Observation (TECO-2022)

10-13 October 2022, Paris (France)

USING THE MEASURED PARTICLE SIZE DISTRIBUTION TO ASSESS THE WIND INDUCED UNDERCATCH OF CATCHING-TYPE GAUGES

Arianna Cauteruccio[1,2]; Mattia Stagnaro [1,2]; Luca G. Lanza[1,2]; Pak-Wai Chan[3]

[1] Department of Civil, Chemical and Environmental Engineering, University of Genova, Genova, Italy

[2] WMO Lead Centre on Precipitation Intensity, Genova, Italy

[3] Hong Kong Observatory, Hong Kong, China

Corresponding author: Arianna Cauteruccio, arianna.cauteruccio@edu.unige.it

Abstract:

Many authors highlighted the underestimation affecting catching-type precipitation gauges because of the airflow modification around the gauge when impacted by wind, which deviates hydrometeor trajectories away from the collector. In the present study, a mathematical formulation for the catch ratio (CR) of a typical cylindrical gauge was derived as a function of both wind speed and rainfall intensity from the numerical CR values provided in the literature for various wind speed and drop size combinations. This formulation is used to correct one-minute precipitation measurements obtained from a catching-type cylindrical gauge located at the Hong Kong International Airport field test site. From three years of observations, contemporary wind and drop size distribution measurements obtained from six co-located anemometers and a Two-Dimensional-Video-Disdrometer (2DVD), provided the ancillary variables needed to calculate the Collection Efficiency (CE). A sigmoidal CE curve was obtained as a function of wind speed, while its parameters are found to be related to the rainfall intensity. The data measured by the catching-type gauge during nine rainfall events are then corrected using the derived CE curve as an exemplary application.

1. Introduction

Any precipitation measurement instrument immersed in a wind field acts as a bluff-body and shows an aerodynamic behavior that depends on its geometry. Airflow modifications, when compared with the undisturbed wind field, occur around its body with significant acceleration and vertical velocity components arising especially above the collector (see, e.g., Jevons, 1861). These airflow features deviate the trajectories of the approaching hydrometeors (Cauteruccio, Brambilla et al., 2021), inducing a generally lower efficiency in the collection of precipitation than in the absence of wind.

The wind-induced bias can be adjusted by deriving collection efficiency (CE) curves. In the field, the CE can be calculated as the ratio between the precipitation measured by a gauge in operational conditions and the reference one. A gauge placed in a pit, with the gauge orifice at ground level in order to avoid the impact of wind, is recommended by

WMO as a reference for liquid precipitation (for additional details see Cauteruccio, Colli et al., 2021).

CE curves are also numerically derived (see e.g. Cauteruccio and Lanza, 2020 for liquid precipitation and Cauteruccio, Chinchella et al. 2021 for solid precipitation). The numerical approach is based on computational fluid dynamics (CFD) simulations to establish the airflow patterns (acceleration, velocity components, and turbulence intensity) produced by the bluff-body behavior of the gauge and a Lagrangian particle tracking (LPT) model to calculate hydrometeor trajectories in such disturbed conditions.

The LPT model allows to calculate, per each particle size/wind speed combination, the catch ratio CR, defined as the ratio between the number of particles captured in disturbed airflow conditions and the maximum number of particles that would be captured in undisturbed conditions. After introducing a suitable drop size distribution (DSD), indicating the number of particles (N(d)) per unit volume of air and per unit size interval having volume equal to the sphere of diameter d, the integral of the CRs over the range of diameters provides the numerical CE. DSD measurements are available thanks to the employment of non-catching type gauges, also called disdrometers.

In this work, CE curves were derived using DSD data from three years of measurements performed at the field test site of the Hong-Kong International Airport thanks to the availability of a two-dimensional video disdrometer (2DVD), together with wind speed measurements. Results were employed to correct rainfall intensity measurements obtained from a catching type gauge during nine sample rainfall events.

2. Methods

Cauteruccio and Lanza (2020) provided the CR values for a catching-type cylindrical gauge as a function of the drop size (d) and wind speed (U_{ref}) obtained by using CFD simulation and a validated LPT model (see Cauteruccio, Brambilla et al., 2021). In the present work, the dependence of those CR values on d was fitted with an inverse second-order polynomial (see Eq. 1)

$$CR(d, U_{ref}) = y_0(U_{ref}) + \frac{a(U_{ref})}{d} + \frac{b(U_{ref})}{d^2} \qquad \text{Eq. 1}$$

The parameters of such curve were expressed as a function of the wind speed as follows:

$$y_0(U_{ref}) = 0.0023 \cdot U_{ref} + 0.9985 \qquad \text{Eq. 2}$$

$$a(U_{ref}) = 0.1106 - 0.113\, e^{-0.4713 \cdot U_{ref}} - 0.0111 \cdot U_{ref} \qquad \text{Eq. 3}$$

$$b(U_{ref}) = -0.1172 + 0.1195 \cdot e^{-0.1944 \cdot U_{ref}} + 0.004 \cdot U_{ref} \qquad \text{Eq. 4}$$

This formulation is adopted here to calculate the CE of a catching type cylindrical gauge based on contemporary wind and DSD measurements. These are obtained at the field test site using six co-located anemometers and a 2DVD, respectively, at a one-minute resolution. DSD measurements were classified as a function of the rainfall intensity (RI) as measured by the 2DVD (see Fig.1). For each RI class, the DSD measurements were fitted using the typical exponential form (Eq. 5), as proposed by Marshall and Palmer (1948):

$$N(d) = N_0 e^{-\Lambda d}$$ Eq. 5

with both parameters N_0 and Λ being a power law function of RI (see Fig. 2).

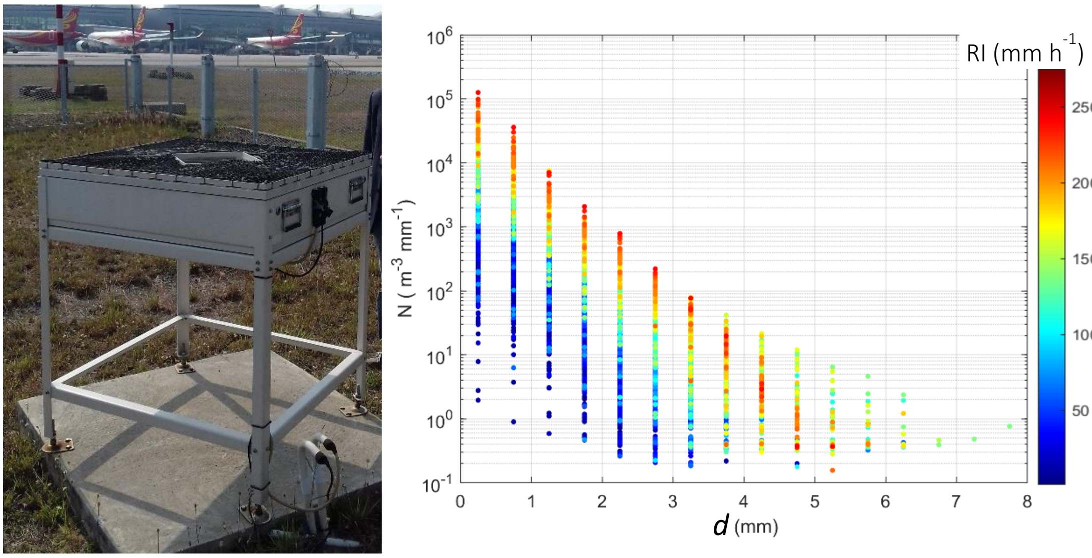

Figure 1: 2DVD installed at the Hong Kong International Airport field test site (left-hand panel) and DSD measurements classified according to the rainfall intensity (see the lateral colour bar).

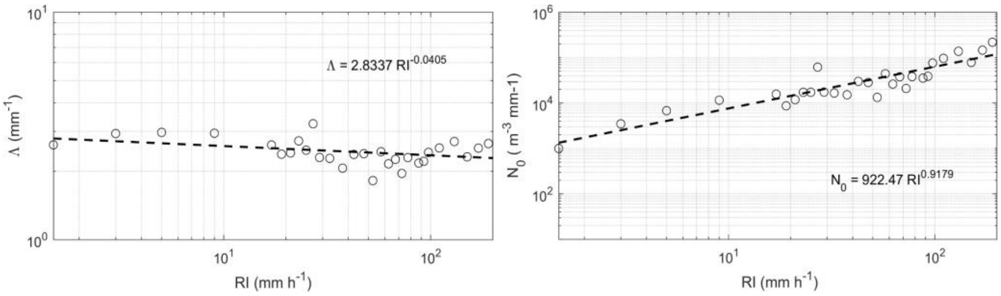

Figure 2: Power law interpolation of the Marshall and Palmer parameters as a function of the rainfall intensity

3. Results and discussion

For each minute of DSD and wind speed measurements, the CE was calculated using the CR and N(d) formulations described in the previous section. Results are graphically shown in Fig. 3 where the size of the circles provides an approximate indication of the RI value (from low RI~1 mm/h with small dots, to high RI~275 mm/h with large circles).

The CE was obtained in the form of a sigmoidal curve (Eq. 6), parameterized with RI, as a function of wind speed:

$$CE\left(U_{ref}\right) = y_0(RI) + \frac{a(RI)}{1 + e^{-\frac{(U_{ref} - x_0(RI))}{b(RI)}}}$$ Eq. 6

Some examples are shown in Fig. 3, where the maximum and minimum values of RI were chosen in order to enclose the entire range of one-minute CE values. It was found that the parameters of the CE sigmoidal curve are related to RI through logarithmic relationships (Fig. 4).

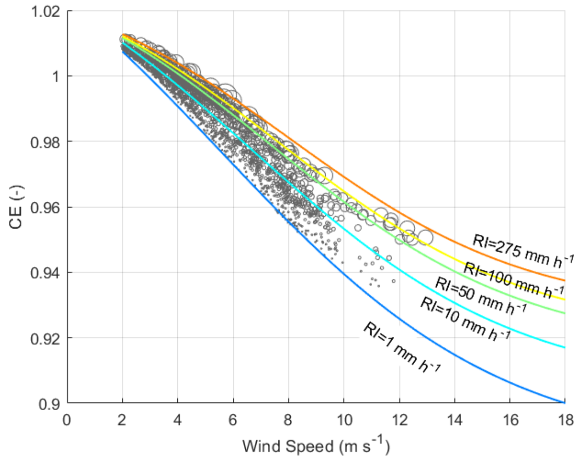

Figure 3: CE values as derived from one-minute DSD and wind speed measurements (black circles) and CE curves at fixed RI values (solid line)

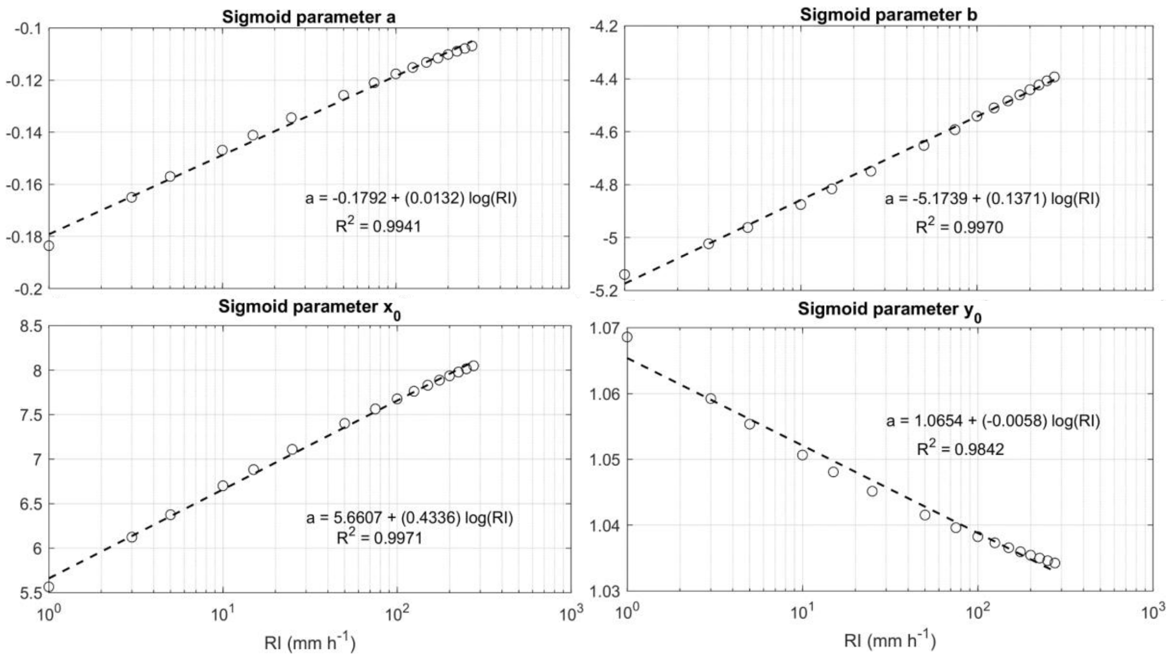

Figure 4: logarithmic relationships between the sigmoidal CE parameters and RI

The derived CE curves allow to correct measurements from catching type precipitation gauges in the absence of contemporary DSD measurements, provided the same climatology and for gauges with cylindrical shape. The direct dependency of the sigmoidal

CE on the wind speed and the derived relationship between its parameters and RI make its practical application quite easy.

An example is summarized in Table 1 where data measured during nine rainfall events by a cylindrical catching type gauge located at the Hong Kong International Airport field test site are corrected. In the table, together with the date of the event, the following information are listed: event duration (h), total amount of rain measured by the catching type gauge without correction (mm), total amount of rain after correction (mm), relative percentage bias between corrected and uncorrected total amount of rain (%), mean and maximum wind speed (m/s).

The maximum obtained bias is about 3.5 % for a mean wind speed equal to 8 m/s. Therefore, the bias at the event scale is limited even in strong wind due to the high percentage of large size drops in the DSD but the correction can be relevant at the seasonal or annual scale.

Table 1: Results of the correction of sample rainfall events

Event	**Duration (h)**	**Tot rain meas (mm)**	**Tot rain corr (mm)**	**Bias (%)**	**Mean wind (m/s)**	**Max wind (m/s)**
22/08/2018	6	50.03	50.63	1.18	4.4	10.4
04/03/2019	13	29.49	30.53	3.41	8.0	11.8
27/05/2019	20	31.21	31.29	0.25	3.3	7.6
13/06/2019	17	52.25	53.30	1.97	5.9	10.7
28/07/2019	4	86.51	87.13	0.71	4.4	8.2
11/05/2020	15	27.74	28.06	1.12	4.1	9.6
18/05/2020	18	30.24	30.97	2.35	5.1	12.9
21/05/2020	6	65.19	65.48	0.44	4.3	6.9
25/05/2020	5	53.22	53.97	1.39	3.9	12.3

4. Conclusions

A suitable formulation of the CR of a given rain gauge geometry (e.g. cylindrical) as a function of the drop diameter, and the dependency of the parameters of such formulation on the wind speed, provide the basis to obtain specific CE functions for any location and rain event characteristics (given the knowledge of the local DSD dependency on the RI obtained from a reference disdrometer). Note that the reference disdrometer is subject to wind-induced biases itself (Nespor and Sevruk, 2000; Chinchella et al., 2021), therefore special care must be posed at obtaining bias corrected DSD measurements.

The mathematical form of the CR as a function of the drop diameter and the wind speed can be obtained by fitting numerical fluid-dynamic simulation results already available in the literature.

Practical use of the proposed method to apply corrections for the wind-induced bias of catching-type gauges is therefore straightforward, and requires no further information than the measured rainfall intensity and the wind velocity (with no need of a disdrometer at each measurement site).

5. References

Cauteruccio, A., Brambilla, E., Stagnaro, M., Lanza, L.G. and D. Rocchi (2021). Wind tunnel validation of a particle tracking model to evaluate the wind-induced bias of precipitation measurements. *Water Resour. Res.,* **57**(7), e2020WR028766. https://doi.org/10.1029/2020WR028766

Cauteruccio, A., Chinchella, E., Stagnaro, M. and L.G. Lanza (2021). Snow Particle Collection Efficiency and Adjustment Curves for the Hotplate Precipitation Gauge. *J. of Hydromet.,* **22** (4), 941 – 954. https://doi.org/10.1175/JHM-D-20-0149.1

Cauteruccio A., Colli M., Stagnaro M., Lanza L.G. and E. Vuerich (2021). In situ precipitation measurements, p. 359 – 400. In: Foken T. (ed.), *Springer Handbook of Atmospheric Measurements*. Springer Nature, Switzerland, ISBN 978-3-030-52170-7, e-ISBN 978-3-030-52171-4, pp. 1740. https://doi.org/10.1007/978-3-030-52171-4_12

Cauteruccio, A. and L.G. Lanza (2020). Parameterization of the collection efficiency of a cylindrical catching-type rain gauge based on rainfall intensity. *Water*, **12**(12), 3431. https://doi.org/10.3390/w12123431

Chinchella, E., Cauteruccio, A., Stagnaro, M. and L.G. Lanza (2021). Investigation of the Wind-Induced Airflow Pattern Near the Thies LPM Precipitation Gauge. Sensors, 21 (14), 4880. https://doi.org/10.3390/s21144880

Jevons, W. S. (1861). On the deficiency of rain in an elevated rain-gauge, as caused by wind. *The London, Edinburgh, and Dublin Philosophical Magazine and Journal of Science*, **21**(4), 421–433. https://doi.org/10.1016/0016-0032(62)90997-3

Marshall, J.S.; Palmer,W.M.K. (1948). The distribution of raindrops with size. *J. Meteorol*., 1948, **5**, 165–166.

Něspor, V.; Krajewski, W.F.; and Kruger, A. (2000). Wind-Induced Error of Raindrop Size Distribution Measurement Using a Two-Dimensional Video Disdrometer. *J. Atmos. Ocean. Technol.*, **17**, 1483–1492.